Eco. Env. & Cons. 28 (August Suppl. Issue) : 2022; pp. (S27-S35)
Copyright@ EM International
ISSN 0971–765X

DOI No.: http://doi.org/10.53550/EEC.2022.v28i04s.005

Sub Surface Structure Modelling Area Around Subdistrict Gantiwarno, District Klatenusing by Gravity Method

M. Irham Nurwidyanto[1], Tony Yulianto[1], Gatot Yulianto[1] and Sugeng Widada[2]

[1]Department of Physic, Faculty of Science and Mathematics, Universitas Diponegoro, Indonesia
[2]Department of Oceanography, Faculty of Fisheries and Marine Sciences, Universitas Diponegoro, Indonesia

(Received 4 June, 2021; Accepted 18 Janaury, 2022)

ABSTRACT

The earthquake that happened on 27th May 2006 in Yogyakarta and its surrounding caused terrible damage as well as thousands of dead victims. Such an earthquake was caused by horizontal Opak's Fault activation and it triggered the emergence of Dengkeng's Fault movement located at the eastern part of the northern Opak's Fault. To mitigate the disaster that might occur in the future, the channel and the condition under Dengkeng's Fault need to be mapped. One of the methods that could be used to recognize the under surface condition is the gravity method which is based on the measurement of gravity field variation on the earth's surface. The existence of a fault would change the condition of rocks in such fault channel zone so that it influences the local gravity change. Therefore, on this opportunity, research of Dengkeng's Fault is carried out using the gravity method. The measurement of the gravity field has been done in 94 points using La-coste Romberg Gravitymeter type G-1118 MVR. The height of the measurement point was measured using GPS Altus APS-3 differential, and the research coordinate was measured using GPS Garmin III Plus. Data on the gravity field that had been obtained was corrected so that complete anomaly Bouguer *(ABL)* is obtained. Further, the regional component of the ABL value is separated from its local component using an upward continuation method. The target that would be identified is shallow so that the local anomaly that would be analyzed uses the second vertical derivative (SVD) and modeled in 3 dimensions using Oasis Montaj software. Second vertical derivative type of fault. 3-dimensional modeling was used to identify the under surface structure of the research area comprehensively. The result of the analysis using the second vertical derivative shows that Dengkeng's Fault is a strike-slip fault with the west-east direction. To clarify the under the surface condition from the 3-dimensional modeling, incisions were made to the Z-axis direction (vertically) and X-axis direction. Z-axis direction modeling shows that the fault in the research area starts to be seen at the depth of 500 meters to 3500 meters to the west-east. X-axis direction modeling shows that the fault was located at Easting 444500 meter and Northing 9141000 meters to the Easting 456250 and Northing 9139000. Based on the modeling result, it could be seen that the southern part block of Dengkeng's moved to the east, while the northern part block moved to the west.

Key words : *Gantiwarno, Dengkeng fault, Gravity method, Second vertical derivative, 3D modeling.*

Introduction

Java is one of the islands in Indonesia located between two plates, i.e. Indo-Australia and Eurasia plates. The island stretches from the east to the west for more or less a hundred kilometers at the north-

ern part of the subduction zone, so that Java Island has some active volcanoes and frequently has a massive earthquake (Gomez *et al.*, 2010).

An earthquake is a seismic vibration coming from the earth caused by the motion of sediment layers under the earth's surface instantly caused by the release of energy accumulation which mostly occurred inside or along the edge of tectonic plates (Shearer, 2009). In Java island, there are some faults on the land and cause a shallow earthquake. One of them is the earthquake attacking Yogyakarta and its surrounding on 27th May 2006. The earthquake killed 5,778 people (from District Klaten 1041), injured 37,883 people, and dozens or even hundreds of thousands of buildings were severely damaged (Bapenas, 2006). The epicenter of the main earthquake was at 8.03 SL -110.32 EL at 05.54 WIB with 5.9 SR and was located at 11.8 km depth (BMG, 2006).

Opak's Fault movement was considered as the cause of the earthquake in such an area (Sulaiman, 2009). Such Opak's Fault stretched from Depok's coastal area to Prambanan in the eastern part of Yogyakarta (Abidin *et al.*, 2006, 2009, Soebowo, 2007). The previous Opak's Fault channel had once been identified using magnet field anomaly data (Fathohah, *et al.*, 2014). Opak's Fault zone modeling had also once been conducted using the gravity method (Irham *et al.*, 2014). The earthquake that occurred in Yogyakarta and Klaten on 27th May 2006, besides it was caused by Opak's Fault movement, it was also considered to be caused by the presence of the contribution of Dengkeng's fault, recalling the huge number of victims around such fault zone. Such fault was at the tip of the northeast of Opak's Fault with strike-slip fault movement caused by Indo-Australia and Eurasia plates subduction under Java Island (Abidin *et al.*, 2009). The existence of Opak's Fault and Dengkeng's Fault could be seen in Figure 1. The 2006 Yogyakarta's earthquake co-seismic deformation horizontal movement was in a range of 10-15 cm (Figure 2). The vector direction of the deformation movement showed a left slide (sinistral). Such co-seismic deformation horizontal slide vector was determined by a GPS survey. It further could be used to estimate the fault geometry of the cause of the earthquake (Abidin *et al.*, 2009). The under the surface condition of Dengkeng's Fault had not been studied thoroughly, especially related to the configuration of the sediment unit faulted. Therefore, in this opportunity, 3-dimensional modeling was conducted using the gravity method.

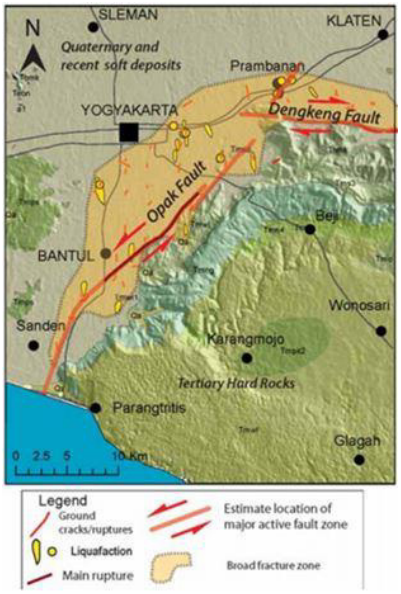

Fig. 1. Opak'sFault and Dengkeng's Fault (courtesy of Natawijaya (LIPI) in Abidin *et al.*, 2009)

This research is expected to be the review on the presence of Dengkeng's Fault that contributes to the cause of damage during the Yogyakarta earthquake and its surrounding. It could also be a reference to mitigating disaster in the fault zone channel and its surrounding area for related institution or community. This is important to recall the possibility of a similar disaster that could happen in the future since the process of the earthquake is a natural cycle.

Study area

The geographical position of the research area was at the coordinate of 110°30′ EL to 110°36′ EL and

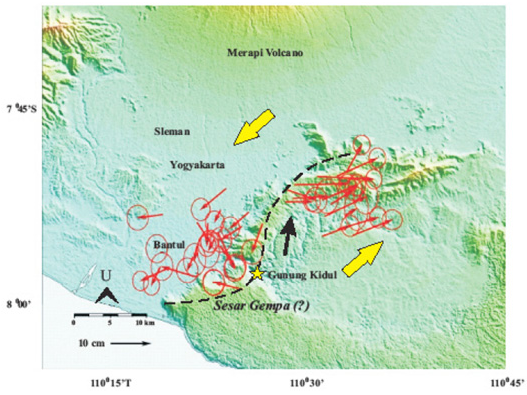

Fig. 2. 2006 Yogyakarta earthquake co-seismic deformation (Abidin *et al.*, 2009).

$7^{0}45'$ SL to $7^{0}51'$ SL in the Geological map shown in Figure 3. The northern part of this research is a lowland composed of volcanic fluvial sediment as the product of Merapi volcano. The southern part is Pematang Baturagung which is a Southern Mountainous channel stretching west-east. From young to old, the lithology of Pematang Batur Agung area consisted of Formation Nglanggran, Semilir, and Kebobutak. Such sediment formation was as old as the early Miocene to Oligocene. The deformation process forming the geology structure of the research area was started in the Pleistocene era (Surono *et al.*, 1992). The geological structure could be found especially in the form of fault stretching west-east to north-south (Samodra and Sutisna, 1997).

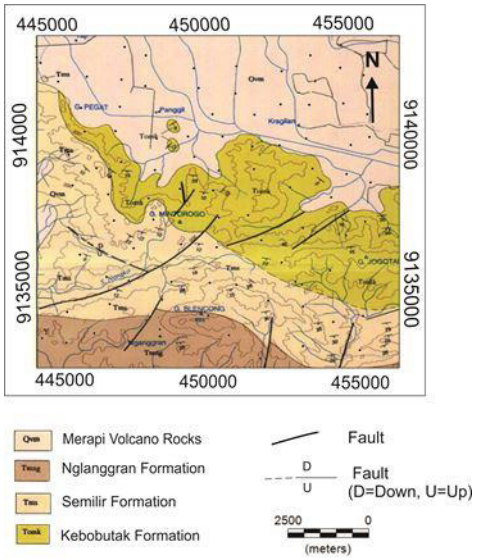

Fig. 3. Geological Map of Research area (Fathonah *et al.*, 2014)

The topography of the research area has the elevation value ranged between 100 meters to 600 meters as shown in Figure 4. The low topography is shown by the blue color located in the north part of the research location, while high topography in the research area is the mountainous channel marked by greenish-blue color. In the southern part, there is Mount Blencong, in the middle there is Mount Mintorogo, in the northwest, there is Mount Pegat, the east part is Mount Jogotamu. The gravity field observed is shown in Figure 5, it has a value distribution of 978113 mGal to 978213 mGal.

Observed gravity field is a gravity field that is actually at the spot. The topography contour map in Figure 4 and the observation gravity contour map in Figure 5 shows the opposite pattern of value. The south, east, and northwest area of the research in the observed gravity field had low value, while in the topography contour pattern in south/east, and northwest of the research area had high value. The higher the topography of an area, the smaller the observed gravity field, and vice versa (Telford *et al.*, 1990)

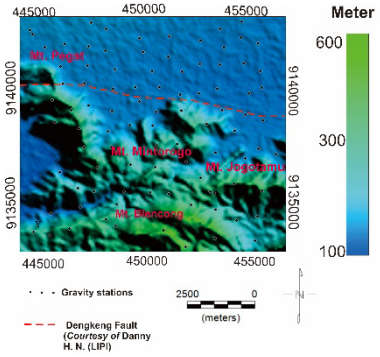

Fig. 4. Topography map of the research area

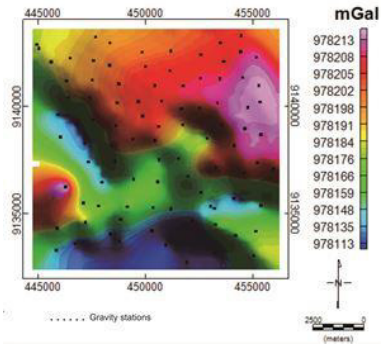

Fig. 5. Observation gravity map of the research area

Data and Methods

Basic Theory

The theory underlying the gravity method is Newton law about universal gravity force. This Newton's gravity law stated that tensile strength between two points of masses m_1 and m_2 with distance r could be written with equation (1) (Telford *et al.*, 1990; Backely, 1995).

$$\vec{F} = -G\frac{m_1 . m_2}{\vec{r}^2}\hat{r} \quad .. (1)$$

with $\vec{F}$ as gravity force experienced by the object (Newton) and G is the gravity field constant ($6{,}67\times10^{-11}Nm^2kg^{-2}$ or $m^3\ kg^{-1}s^{-2}$), m_1 is the mass of object 1 (*kg*), m_2 is the mass of object 2 (5X5T) and $\vec{r}$ is the distance between the center of the mass $m_1$and m_2.

Upward continuation is an upward continuity method aiming to show more regional effect and remove the local effect. The upward continuity method is one of the methods frequently used as a filter to remove noise (Blackely, 1995). The potential field estimation in the field of continuation result (z) could be done using equation (2).

$$U(x,y,z_0-\Delta z)=\frac{\Delta z}{2\pi}\int_{-\infty}^{\infty}\int_{-\infty}^{\infty}\frac{U(x',y',z_0)}{[(x-x')^2+(y-y')^2+\Delta z^2]^{3/2}}dx'dy' \quad .. (2)$$

With U(x,y,z_0) the amount of potential field in the field of continuity result, Äz is the safe distance or the levitation height.

The second vertical derivative could describe the residual anomaly associated with the shallow structure. Theoretically, this method is derived from Laplace's equation shown in equation (3) and (4) (Blackely, 1995).

$$\nabla^2\Delta g=0 \quad .. (3)$$

$$\frac{\partial^2\Delta g}{\partial x^2}+\frac{\partial^2\Delta g}{\partial y^2}+\frac{\partial^2\Delta g}{\partial z^2}=0 \quad .. (4)$$

The second vertical derivative could be used to identify the type of observing fault, reverse fault, or strike-slip fault (Sarkowi, 2012, 2014). The type of fault structure could be shown in the equations (5), (6), and (7).

$$SVD_{maks} > |SVD_{min}| \quad .. (5)$$

The type of granite batholith/intrusion and observe fault, the following equation applies:

$$SVD_{maks} < |SVD_{min}| \quad .. (6)$$

In a strike-slip fault, the following applies (14)]:

$$SVD_{maks} = |SVD_{min}| \quad .. (7)$$

3D modeling was conducted to describe the pattern of the under-surface structure of gravity data by modeling the Bouguer anomaly as the measurement result using inverse modeling (Sarkowi, 2012).

Vertical gravity, g_i, at the 3 dimensions Cartesian coordinate formed with the mass density of $\rho(x', y', z')$ shown in equity (8) (Blackely, 1995).

$$g(x_i,y_i,z_i)=-\gamma\int\int\int\rho(x',y',z')\frac{}{}dx'dy'dz' \quad .. (8)$$

with as the mass density point located at is the Newton gravity constant, and r could be counted using equity (9).

$$r=\sqrt{(x-x')^2+(y-y')2+(z-z')} \quad .. (9)$$

3D modeling was conducted using Software Oasis Montaj with an inverse modeling method. The inverse modeling method needs to discredit under surface area survey into a rectangular prism in which the size and position were identified (Rezai, *et al.*, 2017).

Procedure and Location of research

The research area geographic position was located at the coordinate of 110°30' EL – 110°36' EL and 7°45'SL - 7°51' SL. The distribution of observation spots was 94 with even distribution. The research covered around 11 km x 10.5 km. The data used in this research was the primary data. The gravity field measured with *Lacoste Gravitymeter Type* type G-1118 MVR, while the height of the observation point was measured with APS-3 Altus GPS differential. The data obtained were corrected to find ABL value (complete anomaly Bouguer). Correction performed were: tool height correction, drift correction, tidal correction, latitude correction, free air correction, Bouguer correction, terrain correction to find the value of complete anomaly Bouguer (Teldford *et al.*, 1990; Irham *et al.*, 2019). Terrain correction was performed using SRTM map which had been processed using *Software Global Mapper*and *Oasis Montaj*. Once the value of the Complete Anomaly Bouguer was obtained, the separation of the local and regional anomaly was performed using an upward continuation method (Backely, 1995). The type of fault around the research area could be identified using the Second vertical derivative (Sarkowi, 2012, 2014). Undersurface, modeling was performed using local anomaly modeling. A local anomaly was selected since the area identified was a shallow anomaly (Irham, *et al.*, 2019). Fault information according to Natawijaya and the geology map of the research area could be seen in Figure 6.

Results

The measurement result of the gravity field after the

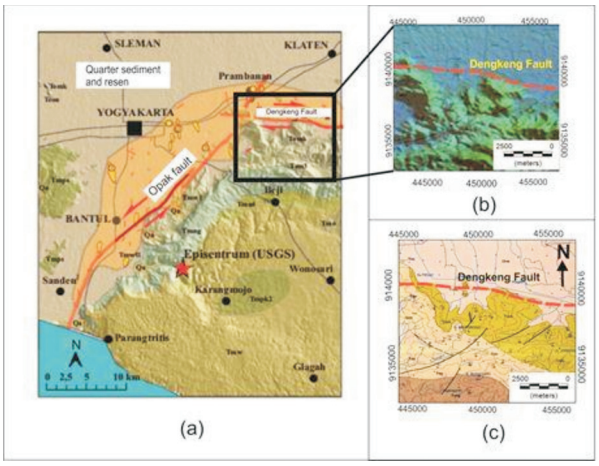

Fig. 6. (a) Fault based on geology map according to Natawijaya (LIPI) (Abidin *et al.,* 2006) (b) SRTM map of the research area (c) Geology map of the research area (Surono *et al.,* 1992).

correction as delivered in the research method was in the form of complete Bouguer anomaly (ABL) ranged between 121 mGal to 176 mGal as shown in Figure 7.

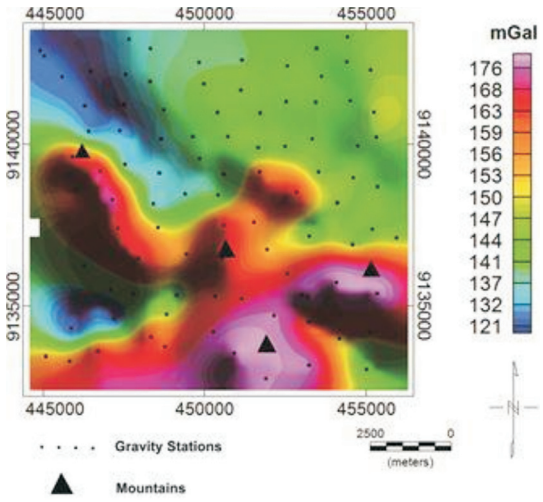

Fig. 7. *Bouguer* anomaly map of the research area

For further analysis, the complete Bouguer anomaly needs to separate its regional and local components. Regional components were associated with the deeper cause and relatively smooth, while local components also known as residual components were associated with relatively shallow and rough. The separation of a regional and residual anomaly in the research area used the Upward Continuation method. (Irham *et al.,* 2019). Such a method was applied up to 4000 meters of height. The result of the upward continuation process was in the form of regional and residual anomaly contour shown in Figure 8 and Figure 9.

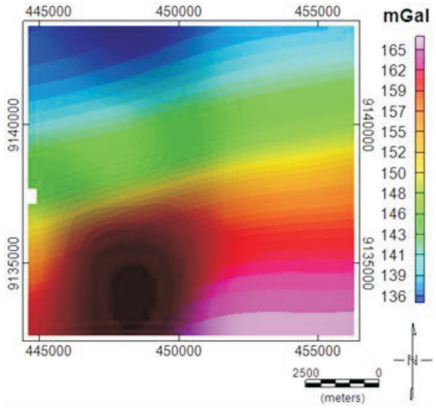

Fig. 8. Regional Anomaly map of the research area

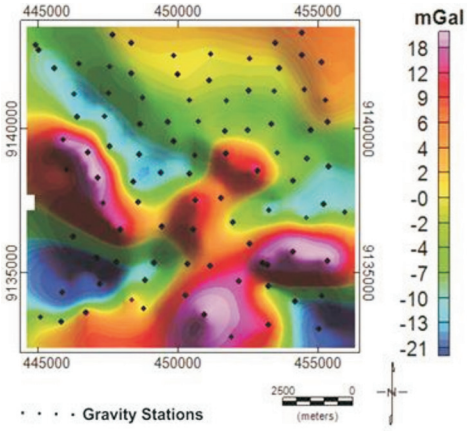

Fig. 9. Residual anomaly map of the research area

The shallow anomaly could be analyzed using the second vertical derivative method (SVD). The contour pattern of the second vertical derivative produced in this research could be seen in Figure 10.

The value of the second vertical derivative in the research area had the value range of 0.0000577 mGal/m^{2}to 0.0000324 mGal/m^2. The second vertical derivative value of zero was the area identified as the fault structure or the limit of sediment contact (Sarkowi, 2014).

The type of fault in the research area could be determined by making an incision through the fault segment as the result of the second vertical derivative interpretation. Such incision is meant to identify the maximum and the minimum value for the iden-

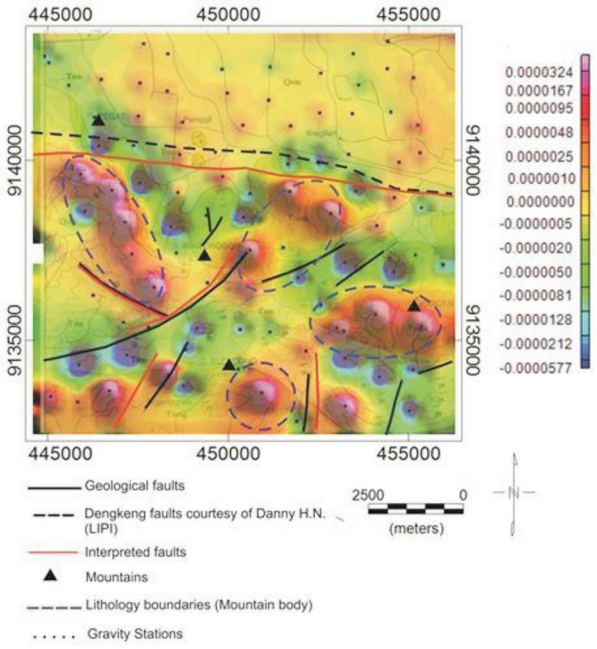

Fig. 10. Second derivative contour with a geology map of the research area

tification of fault type based on the criteria on equations (5), (6), and (7). In this research, the incision was made through A-A′ and B-B′ (Figure 11) with the curve of incision result shown in.

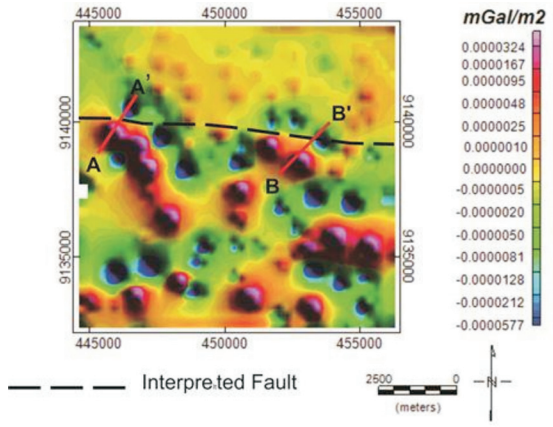

Fig. 11. Incision (red line) on the contour of second vertical derivative

Figure 12 and Figure 13 are the selected incisions to analyze the type of fault in the study area (Sarkowi, 2012)

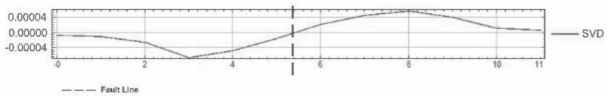

Fig. 12. The curve as the result of incission B-B′second vertical derivative

The analysis of the curve of the result of incision A-A′ second vertical derivative (Figure 12) shows that the maximum value was 1 x 10^{-4} mGal/m^2 and the minimum value of the curve was - 1 x 10^{-4} mGal/m^2. The analysis of the curve of the result of incision B-B′ second vertical derivative (Figure 13) shows that the maximum value was mGal/m^{2}and the minimum value of the curve was -mGal/m^2. The result of the analysis of A-A′ and B-B′ incision curve showed that the maximum and the minimum value of the incision on the contour of the second vertical derivative was the same so that the fault was a strike-slip fault (Sarkowi, 2012).

3-dimensional modeling was conducted to identify the under surface condition. In 3D modeling, the residual anomaly was used recalling the condition expected was a local condition and it was relatively shallow. 3D modeling was carried out using software Oasis Montaj. 3D modeling result was the description of the condition under the surface of the research area based on the density contract as shown in Figure 14.

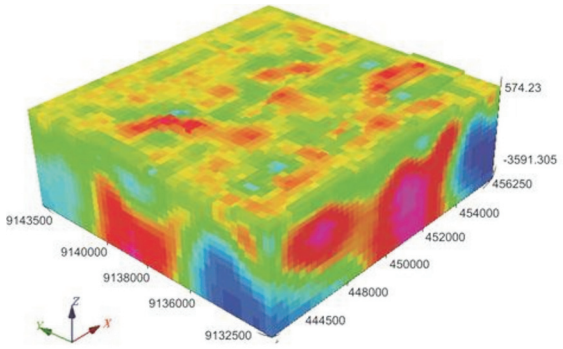

Fig. 14. 3-dimensional modeling in the research area

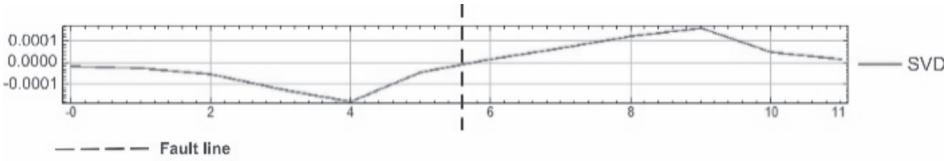

Fig. 12. The curve as the result of incission A-A′second Vertical derivative

3-dimensional modeling result was made an incision on Z and Y-axis in the area identified as a fault. The incision at Z-axis was shown in Figure 15, while the incision at the X-axis was shown in Figure 16 to Figure 19.

Figure 15 (a-h) shows that the image of the 3-dimensional modeling incised at z-axis (upper and lower direction) Figure 15 (a) 3-dimensional modeling was incised at 0 meter depth. At 0 meter depth, the fault had not been able to identify since it was still on the surface. Fault in the research area starts to see at 500-meter depth (Figure 15 (b)) shown by green color contour limiting low contour with blue color and high contour in purple. Incision at 1000 meter (Figure 15 (c)), the fault was clearly seen, the fault was located between the high and low contour. The fault was clearly seen at the depth of 1500 meters (Figure 15 (d)) to the depth of 3500 meters (Figure 15 (h)) under the surface.

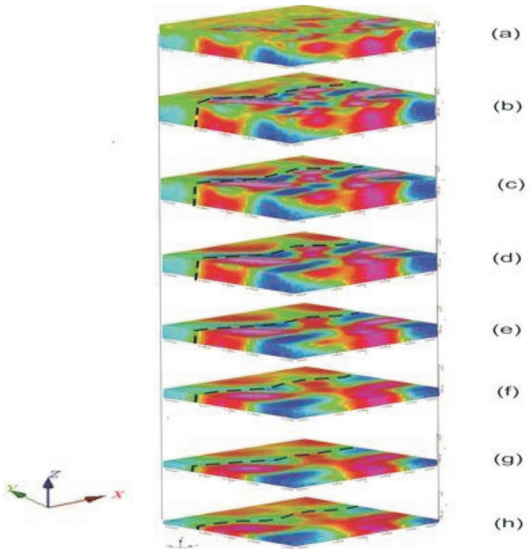

Fig. 15. Incision at z axis of the 3 dimensional modelling. (a) incision at 0 meter depth (b) incision at 500 meters depth (c) incision at 1000 (d) incision at 1500 meter (e) incision at 2000 meter (f) incision at 2500 meter (g) incision at 3000 meter (h) incision at 3500 meter

3-dimensional modeling incised at the x-axis was carried out by cutting the area from the west to the east into 4 incision models. The first incision model was carried out on Easting 447800 (Figure 16). The second incision model was carried out at Easting 450740 (Figure 17). The third incision model was carried out in 451000 (Figure 18). The fourth incision

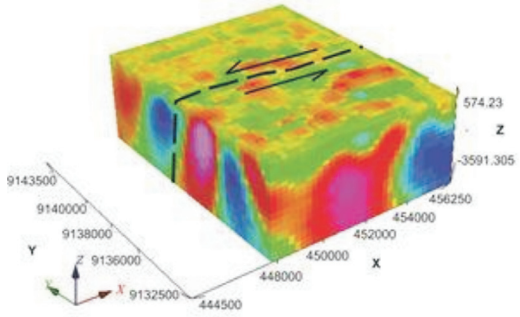

Fig. 16. Incision at Easting 447800

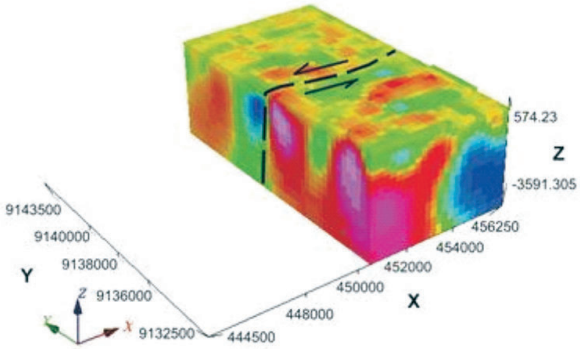

Fig. 17. Incision at Easting 450740

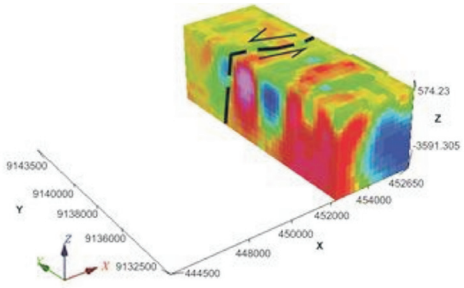

Fig. 18. Incision on 451000

model was carried out at Easting 452400 (Figure 19).

The first incision model (Figure 16) shows that the fault zone in the research result was clearly seen in between the low-density zone and the high-density zone. The Low-density zone was marked with dark blue color and a high-density zone was marked with purple color. The zone that was interpreted as the fault was marked with a dashed black line. The fault zone of the research area in the second incision model (Figure 17) was seen in between the zone with low density and the zone with high density.

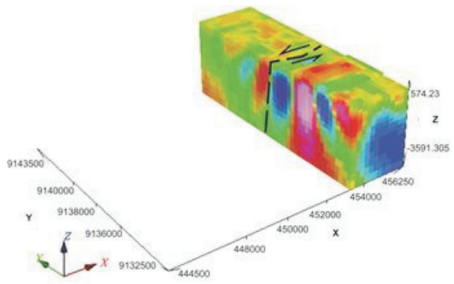

Fig. 19. Incision at easting 452400

The fault was seen in the third incision model (Figure 18), but the low-density zone at that incision was not clearly seen. In the fourth incision model (Figure 19), the low zone started to be seen in the southern part of the high-density zone. The fault zone was identified in between low density and high-density zone as displayed with fault symbol line.

Discussion

Dengken's Fault, based on the analysis result of the second vertical derivative in the west-east direction as shown in Figure 10. The analysis result of the second vertical derivative of the research result could be used to determine the contact limit of the sediment and mountainous formation. The dark blue dashed line is the lithology contact limit of the mountain body. The research area had 4 sediment contact limits considered as the body of the mountain, Mount Pegat in the northwest, the body of Mount Mintorogo in the center, the body of Mount Jogotamu in the east, and the body of Mount Blencong in the south.

The location of Dengkeng's Fault in the research area could be determined using the second vertical derivative analysis. Dengkeng's Fault in geology map and the interpretation result of the second vertical derivative was in the system of 49 S zone UTM coordinates at 444500 meters Easting and 9140000-meter Northing to 456250 meters Easting and 9139000 northing with west-east direction, as shown by the red line in Figure 10.

The direction of the slide of Dengkeng's Fault according to the 3-dimensional modeling showed that the southern part of the Dengkeng's Fault block slide went to the east, while the slide of the northern part of the block of Dengkeng's Fault was to the west. The slide of this Dengkeng's Fault was in line with the co-seismic deformation modeling shown in Figure 2 (Abidin *et al.*, 2009), the direction of Dengkeng's Fault as the result of this research, however, was not in line (went to the opposite direction) from the research result shown in Figure 1. In this case, the author believed that the southern block from the Dengkeng Fault shifted to the east and the northern block shifted to the west since it was also in line with the shift of Opak's Fault as shown in Figure 1 (Abidin *et al.*, 2009), which both intersected the tips. If the southern block of the Dengkeng's Fault shifted to the west then it would collide with the eastern block from the Opak's Fault that went to the north. Such an event would cause folds to occur, while on the topographic display, there were no folds (Irham *et al.*, 2020).

Conclusion

From this research, it could be concluded that in the research area, there had been a fault structure that was interpreted as Dengkeng's Fault. Dengkeng's Fault from SVD analysis was the strike-slip fault. The shift direction of the southern block of Dengkeng's Fault shifted to the east, while the northern part of the block of Dengkeng's Fault shifted to the west. Dengkeng's Fault was in the 49 S zone UTM coordinates from Easting 444500 meter and Northing 9141000 meter to the Easting 456250 meter and Northing 9139000 with west-east direction. The result of the 3-dimensional modeling showed that Dengkeng's Fault started to look at the 500 meters deep to 3500 meters deep under mean sea level.

Acknowledgment

In this opportunity, we would like to express our gratitude to the Chief of LPPM Undip for funding this research, with an agreement of research assignment under a contract number : 474-33/UN7.P4.3/PP/2019.

References

Abidin, H.Z., Andreas, H., Meilano, I., Gamal, M., Gumilar, I. and Idam, A.C. 2009. Deformasi Koseismik dan Pascaseismik Gempa Yogyakarta 2006 dari Hasil Survei GPS. *J Geol Indonesia*. 4(4): 275–84.G.

Badan Meterologi and Geofisika, 2006. Berita Gempa Bumi, Jakarta.

Blackely, R.J. 1995. *Potential Theory in Gravity and Magnetic*

Applications. Cambridge: Cambridge University Press. 441 p 2019.

Buletin Laporan Perkembangan Penanganan Bencana Gempa Bumi Di Jogjakarta dan Jawa Tengah, 2006, No. 32, 3 Juli 2006, 13 halaman ditambah lampiran

Fathonah, I.M., Wibowo, N.B. and Sumardi, Y. 2014. Identifikasi Jalur Sesar Opak Berdasarkan Analisis Data Anomali Medan Magnet dan Geologi Regional Yogyakarta. *Indones J Appl Phys*. 4(2) : 192–200.

Gomez, C., Janin, M., Lavigne, F., Gertisser, R., Charbonnier, S. and Lahitte, P. 2019. Borobudur, a basin under volcanic influence: 361,000 years BP to present. *J Volcanol Geotherm Res*. 2010 Oct; 196(3–4) : 245–264.

Irham, M.N., Sribrotopuspito, K. and Waluyo, Sismanto, 2014. The Sub Surface modeling of Opak Fault Yogyakarta Region With Invertion Method of Gravity data. *International Journal of Basic & Applied Science IJBAS-IJENS*. 14 (06).

Irham, M.N., Yulianto, T. and Widada, S. 2019. Modeling of Semarang Fault Zone using gravity Method. *Journal Of Physics, Conf. Series* 1217 (2019) 012031 IOP Publishing doi : 10.1088/1742-6596/1217/1/012031.

Irham, M.N., Yulianto, T. and Widada, S. 2020. Deliniation Sub Surface Structure of Gantiwarno Subdistrict, Klaten District Using Gradient and Euler Deconvolution Analysis. *ARPN Journal of Engineering and Applied Sciences*. 15 (19): 2057-2064.

Rezaie, M., Moradzadeh, A., Kalate, A.N., Aghajani, H., Kahoo, A.R. and Moazam, S. 2017. 3D modelling of Trompsburg Complex (in South Africa) using 3D focusing inversion of gravity data. *J African Earth Sci.* [Internet]. 130 : 1–7. Available from: http://dx.doi.org/10.1016/j.jafrearsci.2017.03.002

Samodra, H. and Sutisna, K. 1997. Peta Geologi Lembar Klaten, Jawa skala 1: 50.000. In Bandung: Pusat Penelitian dan Pengembangan Geologi; Bandung.

Sarkowi, M. 2010. Identifikasi struktur daerah panasbumi ulubelu berdasarkan analisa data svd anomali bouguer. *J Sains MIPA*. 16 (2) : 111–118.

Sarkowi, M. 2014. Eksplorasi Gaya Berat, Graha Ilmu; Yogyakarta:

Shearer, PM. 2009. *Introduction to Seismology*. Second Edi. United States of Amerika: University Press. Cambridge.

Soebowo, E., Tohari, A. and Sarah, D. 2007. Studi Potensi Liquifaksi di Zona Patahan Opak Patalan Bantul, Yogyakarta, *Prosiding seminar Geoteknologi kontribusi ilmu kebumian Dalam Pembangunan Berkelanjutan, Bandung*. ISBN : 978-979-799-5.

Sulaiman, C., Dewi, L.C. and Triyoso, W. 2008. Karakterisasi sumber gempa Yogyakarta 2006 berdasarkan data GPS. *Jurnal Geologi Indonesia*. 3 (1).

Surono, S., Thoha, B. and Sudarno, I. 1992. Peta geologi lembar Surakarta-Giritontro. Pusat Penelitian dan Pengembangan Geologi, Bandung.

Telford, W.M., Goldrat, L.P. and Sheriff, R.P. 1990. *Applied Geophysics*. 2nd ed. Cambridge University Press. Cambridge.

USGS. Website of the United States Geological Survey (USGS). In 2006. Available from: http://earthquake.usgs.gov/eqcente r/recenteqsww/Quakes/usneb6.php#details